Time-dependent damage analysis for viscoelastic-viscoplastic structural laminates under biaxial loading

Thomas Berton[a], Sandip Haldar[a], John Montesano[b], Chandra Veer Singh[a,c,*]

[a] Department of Materials Science and Engineering, University of Toronto, 184 College Street, Toronto M5S 3E4, Canada
[b] Department of Mechanical and Mechatronics Engineering, University of Waterloo, 200 University Ave. West, Waterloo N2L 3G1, Canada
[c] Department of Mechanical and Industrial Engineering, University of Toronto, 5 King's College Road, Toronto M5S 3G8, Canada

ABSTRACT

Many composite structures are required to sustain severe thermo-mechanical loads over extended periods of time, during which viscoelastic and viscoplastic behavior can cause the progression of micro-damage. In this paper, a new computational multi-scale model that couples micro-damage mechanics with Schapery's theory of viscoelasticity and viscoplasticity has been developed to predict time-dependent damage evolution in laminates under constant biaxial loading. After validation with experimental data, the new model capabilities are showcased by predicting damage evolution in two distinct laminates under different axial and transverse loads over time. It is found that damage evolution in both laminates is highly sensitive to the biaxial loading levels, and that crack multiplication in each ply is dependent on stacking sequence and ply orientation. The developed multi-scale model may be a suitable design tool for composite structures required to endure long-term loads in demanding environments.

1. Introduction

Composite laminates are increasingly used as structural components in aerospace, marine, energy, and construction applications due to their high stiffness-to-weight ratios and equivalent mechanical performance to their metallic alloy counterparts [1]. While the stiffness of these materials in the pristine state can be predicted accurately using classical laminate theory, the prediction of progressive failure processes under various loading conditions remains challenging due to the hierarchical structure of fiber-reinforced laminates and the complexity of observed damage modes [2,3]. Moreover, favourable environmental conditions may cause laminates to exhibit significant rate-dependent deformations due to the susceptibility of the polymer matrix [4]. Such behaviour is becoming more important since polymer composites are increasingly used for primary structural applications. For example, aerospace applications of novel composite materials can involve high service temperatures [5], under which these properties of the matrix will be more important. Previous studies have shown that unidirectional glass-fibre and carbon-fibre epoxy plies can exhibit creep behaviour in the transverse and shear directions in which matrix behaviour is dominant [6,7]. Several experimental studies have also found that matrix micro-crack density is affected by the time-dependent properties of the laminates [6,8–10]. Nguyen and Gamby [7], for example, found that for lower

rates of loading, crack density evolution for a given amount of applied stress in a non-linear viscoelastic cross-ply laminate was larger than that for higher loading rates. The authors developed a non-linear time-dependent shear-lag model to interpret this trend, and concluded that the experimental results of crack density evolution for different strain rates were due to the inherently different fracture properties of the matrix. Raghavan and Meshii [9] observed similar results for a cross-ply CFRP. They also studied the evolution of damage during a creep test, and observed that damage could progress under a constant load over time, which had a significant effect on creep strain evolution. Fitoussi et al. studied the effects of matrix viscosity on damage evolution in random glass fiber composites [11] by subjecting a short glass fiber composite to impact loading and monitoring experimentally the evolution of micro-damage mechanisms. They found that increasing the strain rate delayed the onset of damage.

For laminates under tensile loads, ply micro-cracking is usually the first mode of damage and occurs through the nucleation of matrix cracks which rapidly propagate along the width of the laminate parallel to the fibers, and extend through the ply thickness [12,13]. In order to understand the effect of ply micro-cracking, several models have been developed (see [12] for detailed review). These include analytical models such as the shear-lag model [14–16], variational-based methods [17,18], Crack Surface Displacement-based methods [19] and self-

consistent approximations [20]. Continuum Damage Mechanics (CDM) based models, which use experimental data for calibration instead of explicitly modelling the cracked plies have also been developed [21–25].

A more recently developed CDM-based modeling philosophy is the Synergistic Damage Mechanics (SDM) approach, which utilizes computational micro-damage mechanics models to calibrate a CDM model capable of predicting progressive damage [12]. The SDM model is formulated in terms of stiffness degradation parameters describing the reduction of the different components of the stiffness tensor for different matrix micro-crack densities. The stiffness degradation parameters appearing in the SDM model are obtained by calculating the Crack Opening Displacements (CODs) in the different plies of a multidirectional laminate, using a Finite Element (FE) micro-damage model in which cracks are introduced to simulate damage. The SDM model bypasses the costly and complicated experiments that are otherwise required to calibrate CDM models, and can be applied to multi-directional laminates with better accuracy than the analytical methods presented above [26]. The SDM model can be further enhanced by including an energy-based model for crack multiplication, which utilizes the same FE micro-damage model to predict the evolution of crack density for different loading scenarios [27]. Together, SDM and the energy-based damage evolution model can predict stiffness degradation curves describing stiffness loss as a function of loading history. Our recent works on the SDM model have extended its capabilities in several ways. For instance, Berton et al. [28] incorporated the effects of viscoelastic behavior in order to predict the time-dependent response of a CFRP laminate undergoing damage. Singh and Talreja [29] have used the SDM model to make predictions of test cases involving a variety of material systems, stacking sequences, and loading conditions during the recent World-Wide Failure Exercise III. Montesano and Singh [30] extended the model to multi-axial loading scenarios, which will be used here.

The models pertaining to the combined effects of cracking damage and viscoelasticity are few. For example, Ogi and his collaborators [31–33] used a shear-lag model to predict the effect of cracking on the creep response of different laminates. They were able to explain the increase in creep strain with loading and damage evolution. However, time-dependent crack density evolution was not predicted, limiting the applicability of the model. Asadi [34] extended these previous works; he studied the evolution of crack densities in a $[\pm 45/90_2]_s$ laminate in all layers under constant loading. He developed a micro-mechanical variational model to predict damage evolution and performance degradation during constant loading of the laminate. The model was highly accurate, but due to its micromechanical basis, it was restricted to a single stacking sequence. Ahci and Talreja [5] proposed a CDM model accounting for non-linear viscoelasticity and damage to predict the creep response of a cross-ply laminate. This approach required a complicated experimental procedure to determine the parameters of the CDM model, and crack density evolution was not predicted. Varna et al. [35] developed a SDM model accounting for viscoelasticity that could predict stress relaxation of a cross-ply laminate containing cracks. However, crack density multiplication was not predicted, and the analysis was restricted to cross-plies. Giannadakis and Varna [36] proposed a model for predicting the effect of shear damage on the viscoelastic-viscoplastic response of a $[\pm 45]_s$ laminate, which used experimental data to determine the combined effects of damage and time-dependent behaviour on the creep response of the laminate. Al-Rub et al. [37] developed a model combining non-linear viscoelasticity, viscoplasticity and damage to predict the constitutive response of polymers and polymer/clay composites. These last two models were accurate in their combination of separate constitutive models into a single constitutive theory, however experimental calibration involved extensive testing.

In this paper, a new Synergistic Damage Mechanics model has been developed incorporating the effects of biaxial loading as well as non-linear viscoelasticity and viscoplasticity in symmetric laminates to predict progressive matrix microcracking and stiffness loss during constant loading. The viscoelastic-viscoplastic properties of the individual plies based on Schapery's formulation are obtained from the literature, and implemented in the framework of the SDM model to predict damage evolution, and the overall creep response. The model has been validated with respect to experimental measurements published in the literature. The model is capable of predicting micro-crack density evolution in all layers under biaxial loading scenarios in multi-directional laminates, and can also determine the long-term stiffness degradation under different constant loads. Two different laminate sequences, namely $[0/90]_s$ and $[0/90/\mp 45]_s$ have been considered in this study to cover different types of laminates.

2. Progressive Damage Modeling: Synergistic Damage Mechanics (SDM)

The Synergistic Damage Mechanics (SDM) model is a CDM-based damage model that can quantify the stiffness degradation due to sub-critical matrix micro-cracks in the plies of a laminate with a symmetric stacking sequence (which will be referred to as symmetric laminates) which develop under tensile loading. For each ply orientation, the micro-cracks in a given layer will be parallel to the fibers, each orientation corresponding to a specific mode of damage, which is described in terms of a damage tensor. The reduced stiffness due to the matrix micro-cracks can then be calculated with evolving crack densities in the different plies. In SDM, it is assumed that cracks are parallel to each other, equally spaced, span the whole thickness of the ply and the whole width of the representative volume element (RVE) (Fig. 1). Although a given layer may have micro-cracks, it can still carry a load because each micro-crack is constrained by the adjoining plies of the laminate that are oriented at different angles. One of the main advantages of the proposed model is its ability to account for the constraining effects of adjacent plies on the Crack Opening Displacement (COD) of the micro-cracks.

2.1. Synergistic Damage Mechanics (SDM) model

Each mode of damage (α) corresponds to a different ply crack orientation dictated by the ply orientation, and damage in the ply is represented by a damage tensor of the following form:

$$D_{ij}^{(\alpha)} = \frac{\kappa_\alpha t_\alpha^2}{s_\alpha t} n_i n_j \tag{1}$$

where t_α is the thickness of the cracked ply with a given orientation, s_α is the spacing between cracks in the ply, t is the total thickness of the laminate, n_i represents the components of the unit vector normal to the crack surface in the coordinate system of the laminate, and κ_α accounts for the effect of adjacent cracks on the COD of the ply crack. Due to the interactions of the stress fields between cracks in different layers and within the same layer, κ_α will change depending on the crack density of each ply. The stiffness of a laminate that has undergone progressive ply cracking can be defined by:

$$C_{ij} = \begin{bmatrix} \frac{E_x^0}{1-\nu_{xy}^0\nu_{yx}^0} & \frac{\nu_{xy}^0 E_y^0}{1-\nu_{xy}^0\nu_{yx}^0} & 0 \\ \frac{\nu_{xy}^0 E_y^0}{1-\nu_{xy}^0\nu_{yx}^0} & \frac{E_y^0}{1-\nu_{xy}^0\nu_{yx}^0} & 0 \\ 0 & 0 & G_{xy}^0 \end{bmatrix} - \sum_\alpha b_\alpha D_\alpha \begin{bmatrix} 2a_1^{(\alpha)} & a_4^{(\alpha)} & 0 \\ a_4^{(\alpha)} & 2a_2^{(\alpha)} & 0 \\ 0 & 0 & 2a_3^{(\alpha)} \end{bmatrix} \tag{2}$$

C_{ij} is the 3×3 stiffness tensor of a symmetric laminate written in Voigt notation, under plane stress conditions. E_x^0, E_y^0 are the Young's moduli in axial and transverse directions, ν_{xy}^0, ν_{yx}^0 are the major and minor Poisson's ratios, and G_{xy}^0 is the shear modulus of the undamaged laminate. The first term is the stiffness of the undamaged laminate and can be calculated using Classical Laminate Theory (CLT) from the ply properties. The second term represents the reduction in stiffness of the
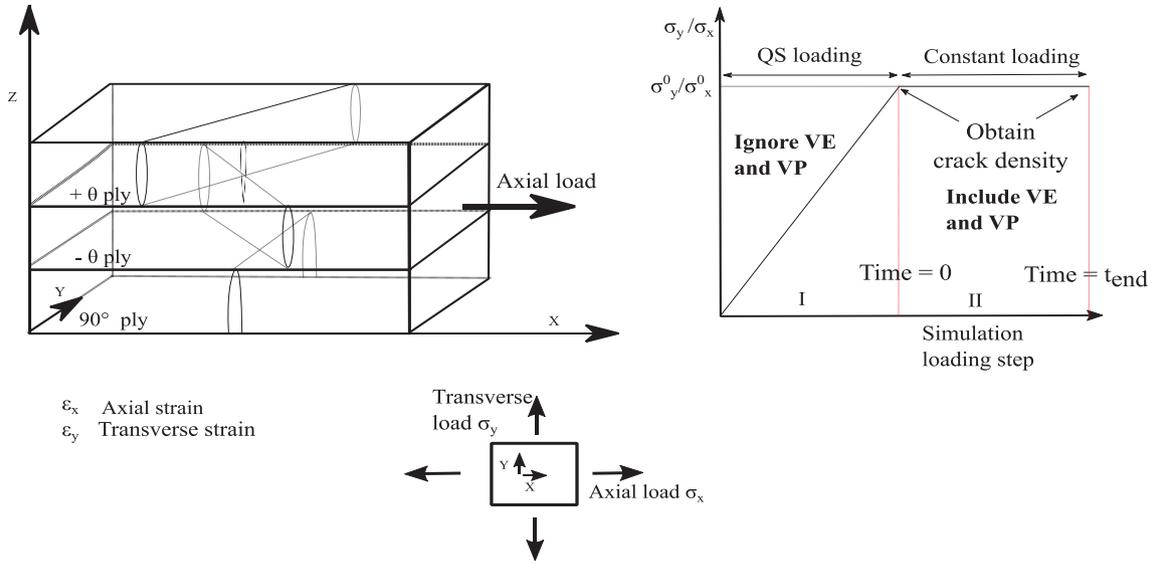
Fig. 1. Schematic showing the different modes of ply micro-cracking in a multi-directional laminate. The top right graph shows the loading scheme used in the current paper. VE refers to the viscoelastic properties of the plies; VP refers to the viscoplastic behaviour; QS is for quasi-static loading.

symmetric laminate due to matrix micro-cracks. It depends on the damage tensor and a set of stiffness degradation parameters $a^\alpha_{[1-4]}$, where there are 4 parameters for each mode of damage α. The parameter b_α depends on the stacking sequence of the laminate, and is equal to 1 for the ply adjacent to the midplane of the laminate and 2 for all other plies. The parameters $a^\alpha_{[1-4]}$ are obtained by computing the change in stiffness of the laminate using FE micro-damage model for a given amount of crack density; they are assumed not to change with increasing crack density. D_α is a scalar which represents the α mode of damage, and is equal to $D_\alpha = \frac{\kappa_\alpha t_\alpha^2}{s_\alpha t}$ (see Eq. (1)). The effect of the cracked ply orientation on the stiffness degradation of the laminate is taken into account through the $a^\alpha_{[1-4]}$ parameters, as well as κ_α, which describes the evolution of COD with respect to crack density in the layer. Note that the indices i and j corresponds to 1, 2 and 6 in Eq. (2), as per Voigt notation, while they correspond to 1, 2 and 3 in Eq. (1).

2.2. FE micro-damage model

The evolution of the COD in terms of the crack density in each layer obtained from FE micro-damage modelling can be calculated as follows:

$$\kappa_\alpha = \frac{(\overline{\Delta u_2})_\alpha}{\varepsilon_{eff} t_\alpha} = \frac{c_1}{1 + (c_2 \rho_\alpha)^{c_3}} \tag{3}$$

where $(\overline{\Delta u_2})_\alpha$ is the average COD, κ_α is the normalized COD, ε_{eff} is the effective strain causing the cracks to open, t_α is the thickness of the cracked ply, ρ_α is the crack density corresponding to the mode of damage α, and c_1, c_2, and c_3 are fitting parameters. These parameters are obtained using FE micro-damage modelling. By varying the crack density and calculating the COD, a relationship between ρ_α and κ_α can be obtained, from which the fitting parameters can be derived. Once the fitting parameters are obtained, the COD can be predicted for a known crack density using Eq. (3). The construction of the FE micro-damage model has been discussed in further detail by Montesano and Singh [30].

In order to by-pass the need for many FE simulations to obtain the COD parameters appearing in Eq. (3), Montesano et al. [38] developed analytical relationships relating these three parameters to the properties of the plies in the laminate. For each ply, these parameters depend on the stiffness of adjacent plies, their orientation, their thickness, as well as on the thickness of the said ply. From these analytical relationships, the obtained parameters can be used for the predictions of the SDM model in Eq. (2). The $a^\alpha_{[1-4]}$ still need to be obtained, however

a single simulation for each component of the stiffness tensor and each ply crack is sufficient to determine these.

2.3. Energy-based crack multiplication model

The SDM model described in the previous section can predict the stiffness degradation for a given state of damage or density of matrix micro-cracks. In order to predict the constitutive response of a laminate undergoing progressive damage, the evolution of the density of matrix micro-cracks is required. The evolution of crack density in each layer of the laminate can be evaluated by using an energy-based model [27].

Based on the evolution of COD with the density of matrix micro-cracks obtained using the FE micro-damage model (Section 2.1), the energy density release rate for crack multiplication can be obtained using the following equation:

$$W_I = \frac{(\sigma_2^\alpha)^2 t_\alpha}{E_2} \left[2\tilde{u}_n^\alpha \left(\frac{s_\alpha}{2} \right) - \tilde{u}_n^\alpha (s_\alpha) \right] \tag{4}$$

Here, $\tilde{u}_n^\alpha(s_\alpha)$ is the normalized COD for a crack spacing s_α (equal to κ_α), E_2 is the modulus in the transverse direction of the ply, and σ_2^α is the local ply transverse stress (perpendicular to the crack surfaces). σ_2^α is calculated based on the local ply strain and the linear elastic properties of the plies. Using the strain energy density release rate calculated with Eq. (4), a numerical procedure implemented in MATLAB is used to predict crack density evolution versus applied global strain on the laminate. In order to predict crack multiplication, the critical energy density release rate G_{Ic} of the ply is required. G_{Ic} is itself calculated based on experimental data on ply cracking, combined with a numerical procedure described in [27]. After the crack density in each layer has been evaluated for a specific point in the loading sequence, the stiffness of the laminate can be determined by using Eqs. (1)–(3). The crack multiplication model accounts for randomness in crack multiplication by defining a stochastic value of the critical energy release rate for crack multiplication G_{Ic} based on a Weibull's function. When calculating crack density, each ply is divided into segments that can undergo cracking. A MATLAB loop calculates a stochastic value of G_{Ic} for each segment to which W_I is compared, and the crack density is adjusted accordingly. Full details of the model are provided in the paper by Montesano and Singh [27].

To incorporate different material models into the framework of the SDM model, the global strain in the material should be determined using the material model. Next, the local stress (σ_2^α) can be computed

from the local strain, which is obtained by transforming the global strain to the ply coordinate system. From there, the energy release rate for crack multiplication can be calculated using Eq. (4), and the crack density can be updated using the approach given above.

It should be noted that the critical energy density release rate for viscoelastic-viscoplastic materials is dependent on loading rate [7,34]. In this work, we determined the G_{Ic} by using experimental data published in the literature [39]. The critical energy for crack multiplication, G_{Ic}, also decreases with time for the time-dependent behaviour of the matrix [40]. In order to determine the form of this decay, an approximate approach was used. Shokrieh et al. [41] obtained a rate-dependent fracture energy for glass fiber composites. The creep strain predicted by the current model was used to calculate the time-dependent creep strain rate. This time-dependent equation was then combined with the strain-rate dependent fracture model of Shokrieh et al. to obtain the decay in $G_{Ic}(t)$. The final form is given by:

$$G_{Ic}(t) = \frac{G_{Ic}^0}{2} + \frac{G_{Ic}^0}{2}\left(\exp\left(-\frac{t}{10^4}\right)\right)^{0.807} \quad (5)$$

where G_{Ic}^0 is the critical energy for crack multiplication at time t = 0 (start of constant loading) and t is time since the start of the creep simulation.

It should be noted that in this part of the model, the time-dependent properties of the matrix are accounted for through the time-dependent $G_{Ic}(t)$, and the time-dependent COD evolution. The ply properties are assumed to be linearly elastic. This is deemed reasonable given that the stress relaxation caused by the time-dependent behavior of the matrix are very small. Independent calculations showed that ply stress relaxation does not affect crack multiplication significantly.

2.4. Material models for viscoelasticity and viscoplasticity

The creep strain of a viscoelastic-viscoplastic ply can be calculated as a function of time for different constant loading levels using Schapery's thermodynamics-based constitutive model [42]. The creep strain can be defined using the following equation [43]:

$$\varepsilon_i(t) = \left[A_0 + \sum_{r=1}^{k} A_r\left[1 - e^{-\frac{t}{\tau_r}}\right]\right]\sigma_i + \zeta_{ki}(\sigma)\xi(t)\sigma_i \quad (i = 2, 3) \quad (6)$$

where $i = 2$ for the transverse strain component, and $i = 6$ for the shear strain component. The first term in square brackets represents the viscoelastic response of the material. In the material system studied here, Megnis and Varna [43] showed that the viscoelastic deformation could be assumed to be linear. The summation term corresponds to a Prony series consisting of k terms, where A_r is the increase in time-dependent compliance corresponding to the rth term of the Prony series, and τ_r is the time-constant describing the rate of increase in compliance with time. The second term in Eq. (6) represents viscoplastic strain expressed in the form of the product of a stress-dependent function, and a time-dependent function. The exact expressions for these functions are given by: $\zeta_{66} = 5.974 \cdot 10^{-9}\tau_{12}^2 + 3.419 \cdot 10^{-8}\tau_{12} + 3.621 \cdot 10^{-7}$ where τ_{12} is the shear stress in MPa, and $\xi(t) = 0.003t^{0.43}$. We should note that according to the experimental study [43], viscoplastic deformation only occurred in the shear direction. Following the implementation of Eq. (6) for each ply, a numerical procedure developed by Dillard et al. [8] was used to obtain the viscoelastic-viscoplastic behavior of the laminate from the viscoelastic-viscoplastic behavior of the individual plies.

2.5. Combined laminate time-dependent behaviour and damage evolution

The present work is concerned with the progression of damage during constant loading, and the resulting creep strain. Under constant loading, the crack density in the different plies of the laminate will continue to increase as a result of increasing strain. The model calculates the effect of damage on the time-dependent behaviour through the following strain formulation:

$$\varepsilon_i^L(t) = S_{ij}^L \sigma_{CONST,j}^L + \varepsilon_{CREEP,i}^L \quad (7)$$

In Eq. (7), $\varepsilon_i^L(t)$ is the time-dependent strain tensor that includes the effects of damage (with 3 components as per the plane-stress approximation, and in Voigt notation). The first term is the elastic part of the strain under a constant load $\sigma_{CONST,j}^L$ and depends on the number of micro-cracks that dictates the decrease in laminate compliance S_{ij}^L due to damage. The decrease in laminate compliance is obtained using the SDM model using Eqs. (1)–(3) [28]. Under constant loading, the increase in local ply strain will lead to an increase in the crack density and COD. The increase in crack density under constant loading will increase the state of damage, thereby enhancing the creep response through its effect on the elastic component of strain, as per Eq. (7). Therefore, viscoplasticity will affect the damage evolution and the total creep strain in two ways. First, the viscoplastic strain will cause an increase in the local ply strain during loading, which will increase the time-dependent crack density. Second, the viscoplastic strain will directly increase the total creep strain relative to that in a system that is purely viscoelastic.

2.6. Numerical implementation

The SDM model with viscoelastic-viscoplastic material model has been implemented in MATLAB and the loading scheme is explained in Fig. 1. A flowchart explaining the MATLAB algorithm for calculating damage during quasi-static and constant loading is also shown in Fig. 2. The simulation was performed in two steps, (a) quasi-static loading and (b) constant loading. At each simulation step, the local energy density release rate for crack multiplication was calculated using Eq. (4). The crack density was then updated when the energy release rate for crack multiplication (W_I) was found to be higher than the critical energy release rate for crack multiplication (G_{Ic}) [27]. Using the SDM model, the stiffness of the laminate can then be updated, and the stress–strain response predicted. The axial and transverse loads are increased to their respective constant load levels (σ_x^0 and σ_y^0). Following the quasi-static loading, the loads were maintained constant. A similar procedure was followed for time stepping during the creep deformation except that the time dependent critical energy release rate for crack multiplication ($G_{Ic}(t)$) was used to determine the crack multiplication and the viscoelastic-viscoplastic material model was used to predict strain. Once the crack density was updated, the stiffness was calculated using Eqs. (1)–(3), and the total creep strain updated as per Eq. (7).

3. Results and discussion

3.1. Model validation

In order to demonstrate the accuracy of the current model, and its ability to predict the time-dependent behavior of viscoelastic-viscoplastic composites, the model has been validated with respect to experimental data, as well as previous models. Due to the current unavailability of experimental data for time-dependent matrix microcrack multiplication in viscoelastic-viscoplastic laminates, the different components of the model have been validated separately. The three parts of the model were presented in Section 2, and consist of a viscoelastic-viscoplastic material model for laminates (not including the effects of damage), a time-dependent micro-crack multiplication model, and a stiffness degradation model based on Synergistic Damage Mechanics.

3.1.1. Validation of the viscoelastic-viscoplastic implementation

We first validate the nonlinear viscoelastic-viscoplastic model, without any damage, by comparing the predictions from our implementation to the theoretical creep simulation results for a GFRP laminate under uniaxial loading previously published by Megnis and
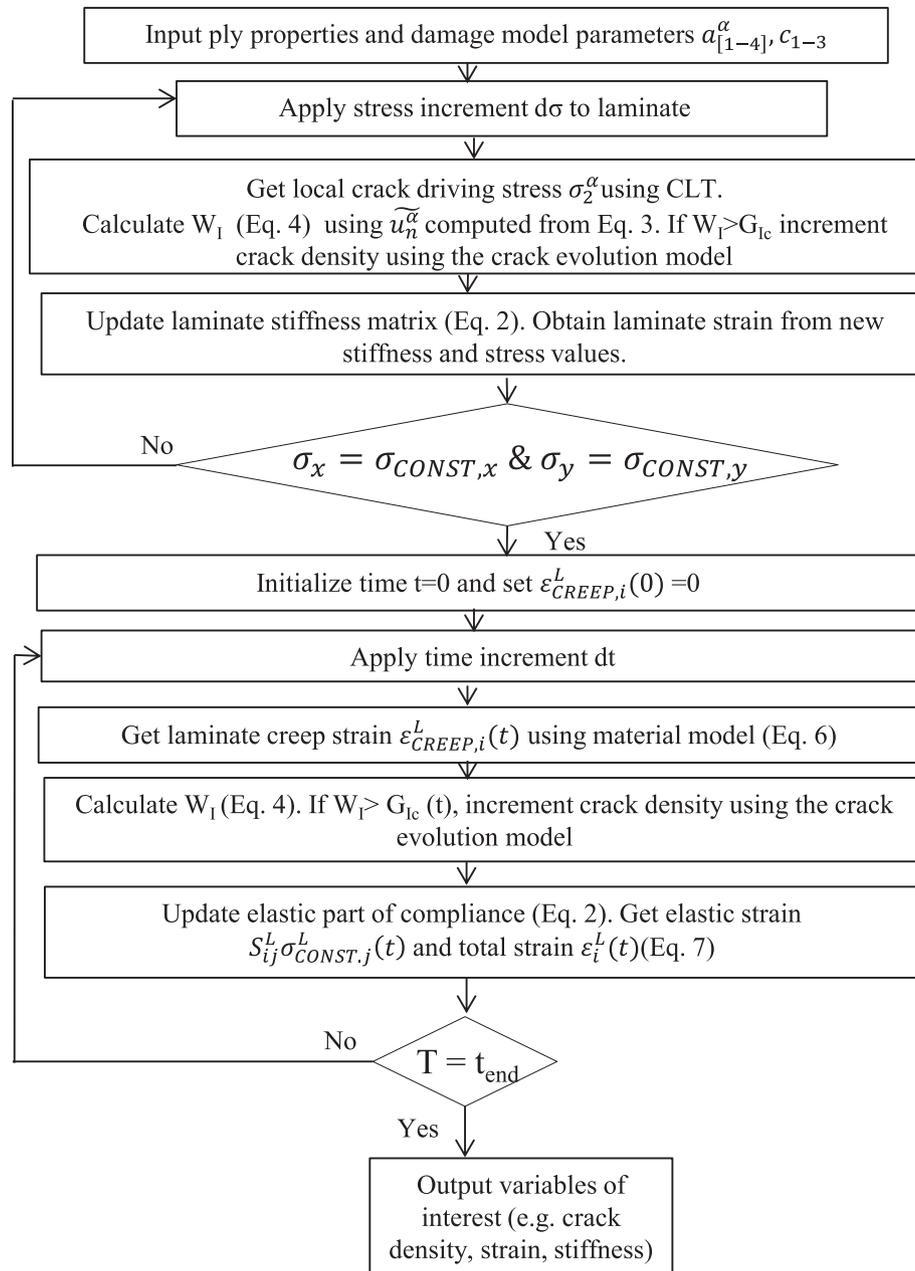
Fig. 2. Flowchart explaining the MATLAB program used to perform the progressive damage simulations under viscoelastic-viscoplastic creep.

Table 1
Parameters for the viscoelastic part of the model [42].

	A_1 (Pa^{-1})	A_2 (Pa^{-1})	A_3 (Pa^{-1})	A_4 (Pa^{-1})
Transverse	8.12×10^{-12}	2.81×10^{-12}	6.14×10^{-12}	8.25×10^{-12}
Shear	3.24×10^{-11}	-3.02×10^{-11}	4.64×10^{-11}	2.29×10^{-11}
τ_r (s)	2400	14,000	25,000	550,000

Table 2
Elastic properties of the plies.

Elastic property	Value
E_1 (GPa)	45
E_2 (GPa)	14.6
ν_{12}	0.32
G_{12} (GPa)	4.95

Varna [43]. The parameters to describe the viscoelastic-viscoplastic behavior of the individual plies of the GFRP laminate as defined in Eq. (6) are given in Table 1 and Table 2. Fig. 3(a) shows the prediction of creep strain following a quasi-static loading to a stress of 50 MPa in the [± 45]$_{2s}$ GFRP laminate and comparison with the material model previously developed by Megnis and Varna for viscoelastic-viscoplastic plies [43]. It can be observed from the figure that the prediction of the current model match very well with the previous work, thus validating the creep model.

3.1.2. Validation of the crack multiplication model

The crack multiplication was validated by comparing its predictions to experimental results provided in the literature for the glass fiber/epoxy material system studied in this paper [39]. The predictions of the crack multiplication model are compared to the experimental data in Fig. 3(b). The critical energy release rates for crack multiplication in each ply were obtained through trial-and-error, until agreement with
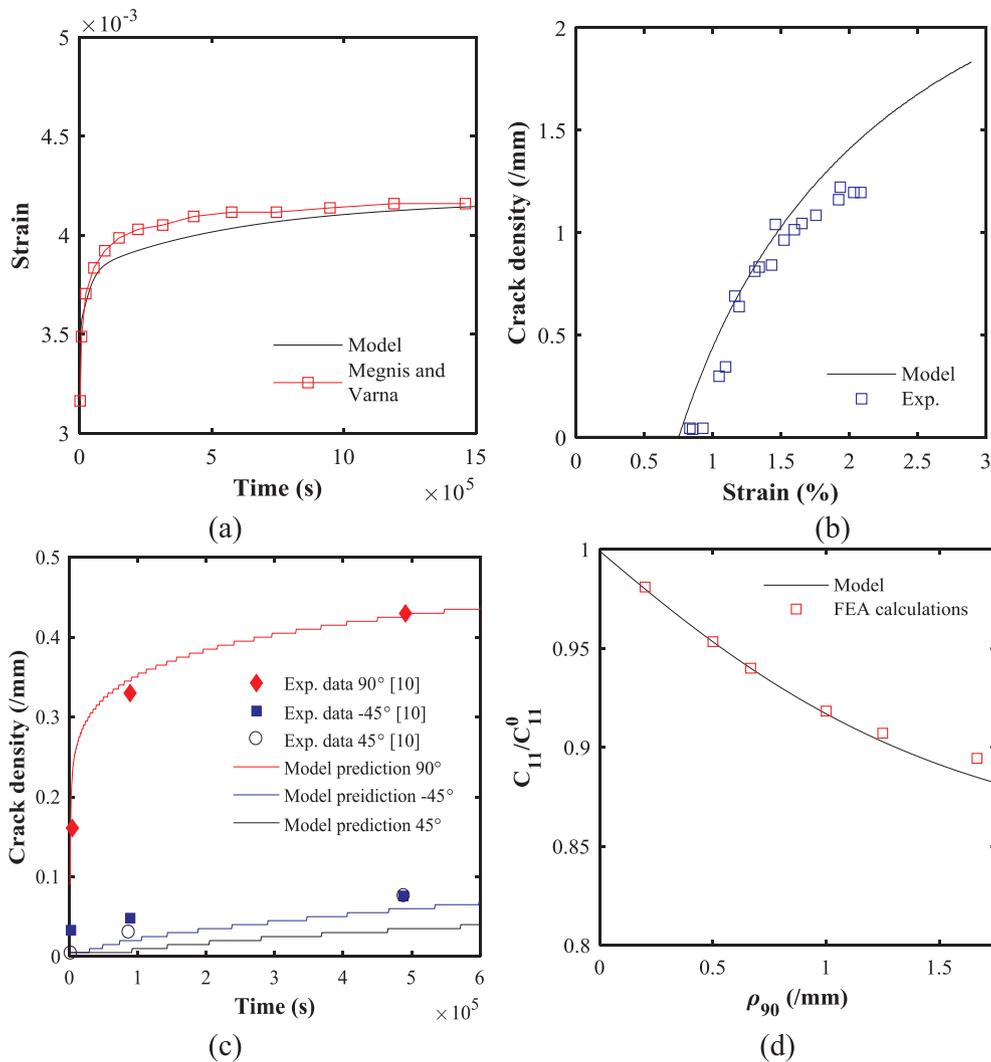
Fig. 3. a) Viscoelastic-viscoplastic creep strain prediction for a $[\pm 45]_s$ GFRP laminate under a creep stress of 50 MPa, and comparison to a previous model from the literature [43]. b) Evolution of crack density under quasi-static loading for a cross-ply GFRP composite, and comparison to experimental data [39]. c) Time-dependent crack density evolution in each layer of a $[\pm 45/90_2]_s$ CFRP laminate predicted by the model, and comparison to experimental data under a creep stress of 45 MPa [34]. (d) Predictions of stiffness degradation with respect to crack density in a $[0/90/\mp 45]_s$ GFPR laminate using the SDM model (Eqs. (1)–(3)) and independent FEA simulations in Ansys Parametric Design Language (APDL).

Table 3
Damage model parameters for glass fiber/epoxy composite.

Laminate		$[0/90/\mp 45]_s$				$[0/90]_s$	
Ply orientation		0°	90°	−45°	45°	0°	90°
Stiffness degradation parameter (GPa)	a_1	0.77	8.08	5	5	0.77	8.14
	a_2	7.45	0.84	4.92	5.01	7.55	0.82
	a_3	1.74	1.54	0.90	0.84	1.30	1.61
	a_4	4.78	5.37	3.48	2.56	6.64	3.07
Critical energy release rate	G_{Ic}^0	300	300	300	300	300	300
COD evolution parameters	c_1	3.15	1.28	1.28	1.26	3.15	1.26
	c_2	0.95	0.35	0.35	0.7	0.95	0.7
	c_3	1.69	1.63	1.63	1.61	1.69	1.61

experiments was satisfactory. The values G_{Ic}^0 for each laminate and each ply are given in Table 3. In one of our previous publications [27], a computational procedure was developed for obtaining G_{Ic}^0 based on the ply crack initiation strain only, bypassing the trial-and-error approach. However, such a procedure is complicated and time-consuming, and since the focus of the present paper is on time-dependent damage

evolution, we have used the trial-and-error method instead.

In the case of the simulations performed in this paper, it was necessary to predict the evolution of cracking during constant loading. As explained in Section 2, this was accomplished by implementing a time-dependent critical crack multiplication energy, $G_{Ic}(t)$ (Eq. (5)). Using this time-dependent critical energy, as well as the creep model for viscoelastic-viscoplastic composites, crack multiplication was predicted for a $[\pm 45/90_2]_s$ CFRP laminate for which time-dependent micro-cracking has been studied experimentally by Asadi [34]. The results of the model have been compared to the experimental measurements in Fig. 3(c), showing almost perfect agreement.

3.1.3. Validation of the SDM model

The stiffness degradation parameters used for the SDM model, namely a_{1-4}^α, were obtained for the GFRP laminates using FEA micro-mechanical simulations and are provided in Table 3. The parameters for the evolution of COD with respect to crack density are provided in Table 3 as well. In order to validate the SDM model for the GFRP, independent FEA simulations were performed for different crack densities from which stiffness was obtained. The predictions of the independent FEA simulations were compared to the predictions of the SDM model, as shown in Fig. 3(d). Clearly, the predictions of the SDM model are
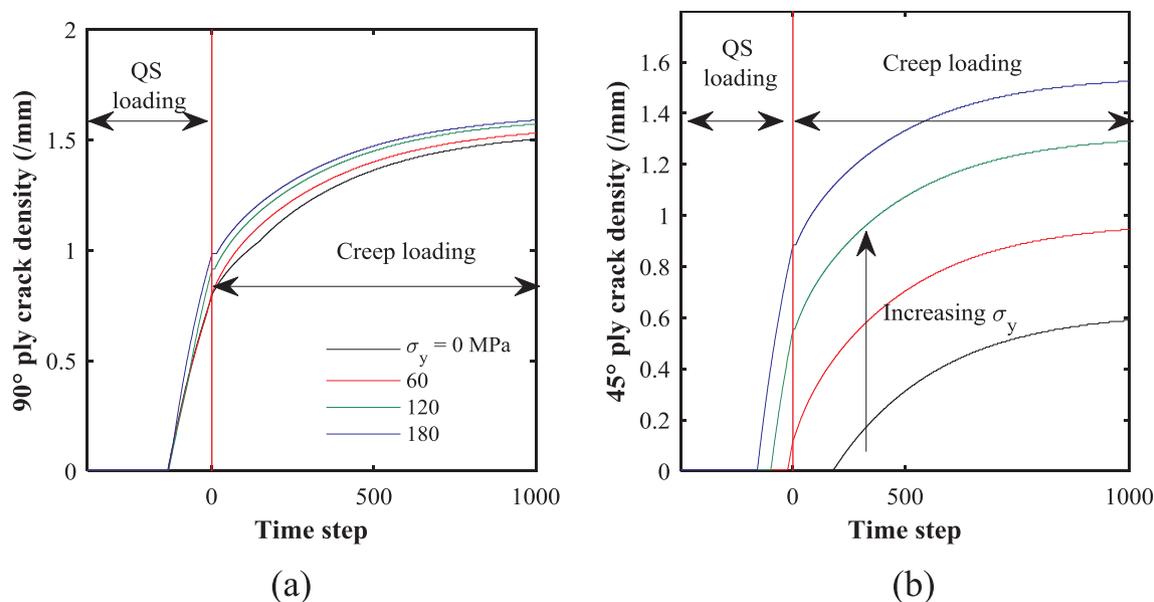
Fig. 4. Crack density evolutions versus simulation time for a $[0/90/\mp45]_s$ GFRP laminate loaded to an axial load of 210 MPa. a) 90° ply crack density. b) 45° ply crack density.

extremely close to the independent simulation results, thus validating the analytical COD formulation, and the $a_{[1-4]}^{\alpha}$ parameters.

3.2. Model predictions

Two laminates with different stacking sequences and the same ply material properties were considered in this work to investigate the effect of ply lay-up. A detailed parametric study has been performed to predict the crack density and stiffness degradation in the $[0/90/\mp45]_s$ and $[0/90]_s$ glass fiber/epoxy laminates with viscoelastic-viscoplastic properties described by Eq. (6) and material properties obtained from Megnis and Varna [43]. The parameters for the energy-based crack multiplication model and the SDM model are given in Table 3. The ply thickness was set to 0.5 mm.

Fig. 4(a) shows the evolution of crack density in the 90° ply of a $[0/90/\mp45]_s$ CFRP quasi-isotropic viscoelastic-viscoplastic laminate during quasi-static and under creep deformation at a constant axial load of 210 MPa. The different curves correspond to different transverse loads. The initial portion of the curves to the left of the red vertical line corresponds to the quasi-static loading, while the portion to the right of the red line corresponds to the constant load simulation. It can be observed from the figure that cracking initiates during the quasi-static loading, and the crack density continues to increase during the creep test. The crack density evolution shown in Fig. 4(a) can also be qualitatively compared to experimental measurements of crack density evolution during constant loading (see [6]). From Fig. 4(a), it can be seen that an increasing applied transverse stress σ_y does not lead to a large difference in crack density evolution in the 90° layer. The crack density in the 90° ply reaches approximately 1.5 cr/mm at long times under all transverse loads. The evolution of crack density in the $+45°$ ply is shown in Fig. 4(b). The overall trends of the evolution of crack density are similar to that in the 90° ply. However, transverse loading has a large effect on the crack density in the off-axis ply. This effect is due to the orientation of the plies for which a transverse laminate stress causes a larger local transverse stress driving crack multiplication. The crack density is equal to 0.6 cr/mm under uniaxial loading in the 45° ply, while it reaches 1.5 cr/mm under a transverse load of 180 MPa.

To quantify the increase in crack density during creep deformation under biaxial loading, crack densities before (t = 0) and after (t = t_{end}) the viscoelastic-viscoplastic deformation are shown in Fig. 5 for the 90° and $-45°$ plies of the $[0/90/\mp45]_s$ quasi-isotropic laminate. In the case

of the 90° ply, the crack density increases with the applied axial load σ_x, with crack initiation occurring at around 140 MPa, as can be seen in subplot (a). The effect of creep strain is to lower the stress necessary to reach a given crack density, shifting the crack initiation stress to around 80 MPa, as can be seen in subplot (a). The transverse load has very little effect on the crack density evolution, both before and after constant loading. This can be explained from the stacking sequence of this laminate. In the case of the 90° ply of the quasi-isotropic laminate, the transverse load causes a slight contraction of the laminate in the axial direction, preventing cracking. However, the out-of-plane contraction enhances crack multiplication. In this particular stacking sequence, these effects cancel out, such that the transverse load has almost no effect on crack density evolution in the 90° ply. In the case of the $-45°$ ply, shown in subplot (b), the crack density also increases with increasing axial stress. The transverse stress has a very large effect on the crack initiation stress, however, reducing it from more than 240 MPa to about 80 MPa at time t = 0, and from 150 MPa to less than 0 MPa at time t = t_{end} as seen in subplot (b). This can be explained from the fact that the transverse stress causes an increase in the local ply COD and local transverse stress by increasing the local ply transverse strain. After creep deformation has occurred, the crack density in the $-45°$ ply has significantly increased.

To show the effect of biaxial load ratio crack density evolution and stiffness, the evolution of crack density in the different plies of the $[0/90/\mp45]_s$ laminate and its axial and transverse stiffness with respect to the biaxial load ratio are shown in Fig. 6(a). The results correspond to an axial load σ_x level of 150 MPa and a varying transverse load σ_y of 0–300 MPa. It can be seen for the quasi-isotropic laminate that the crack density in 45° and $-45°$ plies are most affected by the transverse load. While the crack density in 90° ply increases from 0.9 to 1.15 cr/mm, the crack density in $-45°$ ply increases from around 0 cr/mm to more than 1.7 cr/mm. As expected, the increase in transverse load significantly affects the transverse stiffness as can be seen in the figure. It also affects the axial stiffness significantly, leading to a decrease in modulus from 0.91 to 0.7 of the initial value. In the case of the cross-ply laminate shown in subplot (b), crack density in both layers increases due to transverse load, leading to more severe stiffness degradation in both laminate directions. The predictions of crack density evolution up to around 0.8 cr/mm and associated stiffness degradation by 20% in these laminates are in good agreement with experimental observations [44]. We should note that the results of Fig. 6 are taken at the end of the
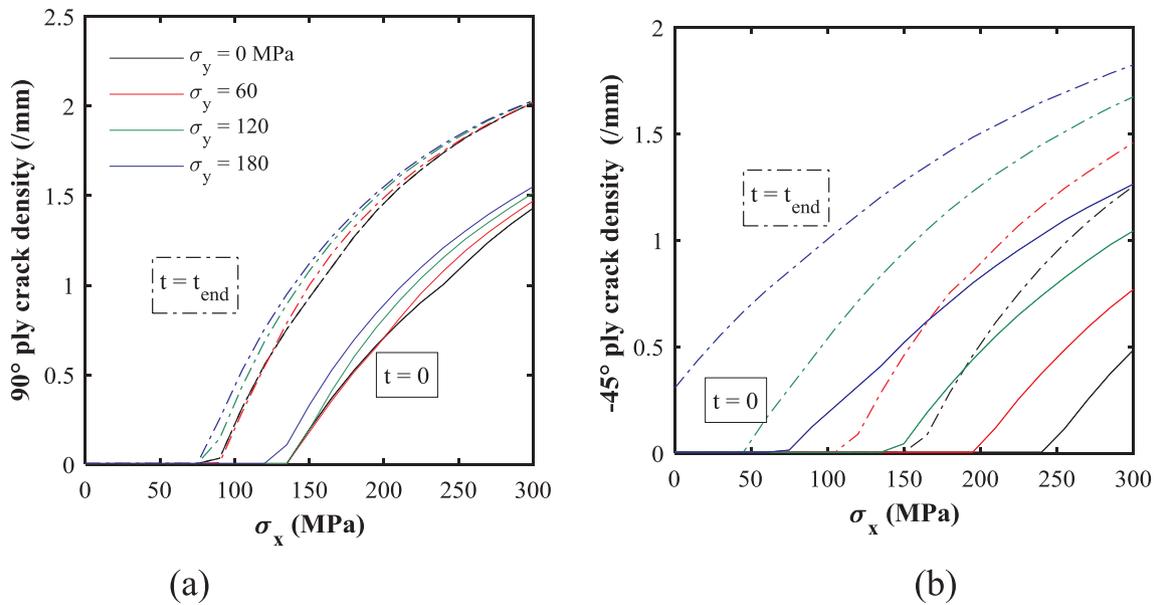
Fig. 5. Crack density versus axial stress with different levels of transverse stress in the 90° and 45° plies of the quasi-isotropic GFRP $[0/90/\mp45]_s$ laminate before (t = 0) and after (t = t_{end}) creep deformation.

creep simulations.

The axial stiffness due to damage progression under quasi-static loading (i.e. before creep) and that under constant loading is depicted in Fig. 7 for the two GFRP laminates. The solid lines represent the stiffness of the laminates after quasi-static load, i.e. before creep deformation, and the dashed lines represent the stiffness of the laminates after creep deformation. As can be seen in Fig. 7(a), the initial axial stiffness of the undamaged $[0/90/\mp45]_s$ CFRP starts degrading beyond 140 MPa of uniaxial quasi-static loading and keeps decreasing with increasing applied load. The normalized stiffness reduces to a value of 85% of the undamaged value under a uniaxial load of 300 MPa. Low transverse loads do not have a noticeable effect on damage initiation; however, when the transverse load reaches 180 MPa, damage initiates at an axial load of 80 MPa. Under transverse loading, cracking is enhanced in all layers of the laminate, causing a larger loss in stiffness with axial loading. Under a transverse load of 180 MPa, the stiffness has reduced to 77% of the undamaged value. Creep deformation enhances

cracking, and causes further stiffness degradation. Fig. 7(b) shows the axial stiffness of the $[0/90]_s$ CFRP laminate under quasi-static loading (before creep) and after creep. Under uniaxial loading, the stiffness starts degrading under a load of 150 MPa and keeps decreasing with higher loading levels, due to increased cracking. At the end of 300 MPa of quasi-static loading the axial stiffness reduces to a value of 85% of the initial value. The presence of transverse stress enhances the damage progression leading to a larger reduction in stiffness as can be seen by comparing the solid lines of different colors. Similarly, creep deformation causes further stiffness degradation, with the stiffness reaching a minimum value of 78%, at which point crack density is saturated.

In order to better understand the effects of biaxial loading on stiffness degradation, time-dependent stiffness degradation envelopes have been developed to determine the amount of stiffness loss for different values of biaxial loading in both laminates studied in this paper. In Fig. 8(a), we show the stiffness degradation contour lines in terms of the
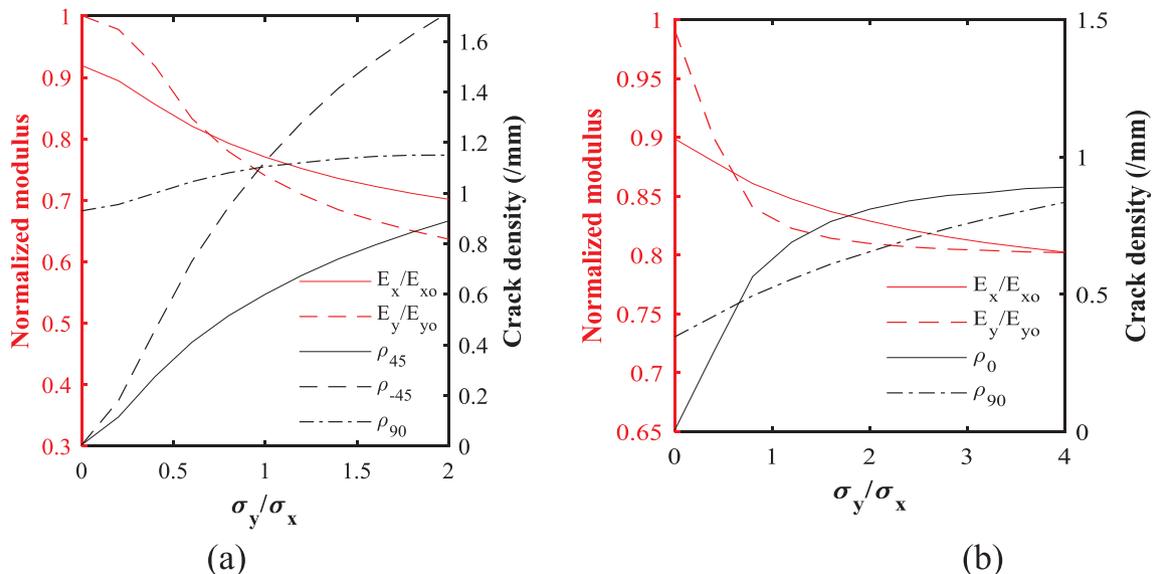
Fig. 6. Evolution of crack density and normalized stiffness for the GFRP composite under different levels of transverse loading: (a) Quasi-isotropic $[0/90/\mp45]_s$ laminate under an axial load of 150 MPa, and (b) cross-ply laminate under an axial load of 150 MPa.
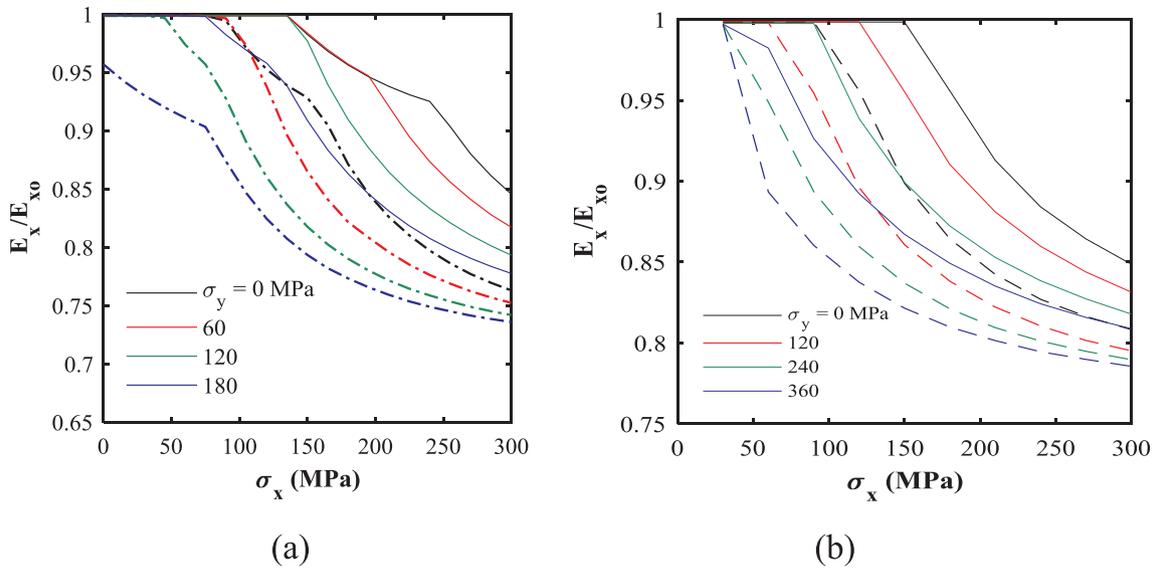
Fig. 7. Axial modulus degradation versus applied axial stress for (a) $[0/90/\mp45]_s$ and (b) $[0/90]_s$ GFRP laminates, at the start of the creep tests, and at the end, for different biaxial loads.

axial and transverse loads for the $[0/90/\mp45]_s$ GFRP laminate, before the creep test, and at the end. In each case, the stiffness degradation contour lines correspond to a loss of 5%, 10% and 15% in the initial axial modulus, E_x^0, or in the initial transverse modulus, E_y^0, depending on which one is greatest. Looking first at the 5% stiffness degradation contour, at time t = 0 (red), we can see that for low transverse loads the line is vertical, showing that the transverse load does not affect crack density evolution. This can be confirmed by inspecting Fig. 5, where it is seen that the crack density in the 90° ply is barely affected by the transverse load. Although the 45° and −45° layer are affected by the transverse load, their effect on stiffness loss at low loads is much lower. Similarly, the 5% contour line is horizontal when the transverse loads are much higher, at which point the stiffness loss is dominated by cracking in the 0° ply. Looking at the trends for the two other stiffness contour lines, corresponding to a loss in stiffness of 10% and 15%, the lines are more slanted. This is due to the effect that transverse loads have on crack multiplication at high loading levels, in the +45° and

−45° layer. From inspection of the stiffness degradation contour lines at the end of the creep simulations, it is clear that the lines have been shifted to much lower values of stress. This suggests that the viscoelastic-viscoplastic properties of the matrix affect the patterns of stiffness degradation under uniaxial loading. For example, the 5% stiffness degradation contour line starts at 125 MPa of axial load, instead of 180 MPa. Under transverse loading, the 5% stiffness degradation contour line crosses the vertical axis at 80 MPa when viscoelastic-viscoplastic deformation has been taken into account, while it only crosses the axis at 120 MPa when creep viscoelastic-viscoplastic deformation is ignored. These marked effects are due to two factors which affect the multiplication of micro-cracks in the different plies of the laminate. First, viscoelastic-viscoplastic deformation increases the driving force for crack multiplication by increasing the amount of strain for a given applied load. Second, under time-dependent deformation, the critical energy release rate for crack multiplication (see Eq. (5)) degrades due to the behavior of the matrix, which enhances crack multiplication
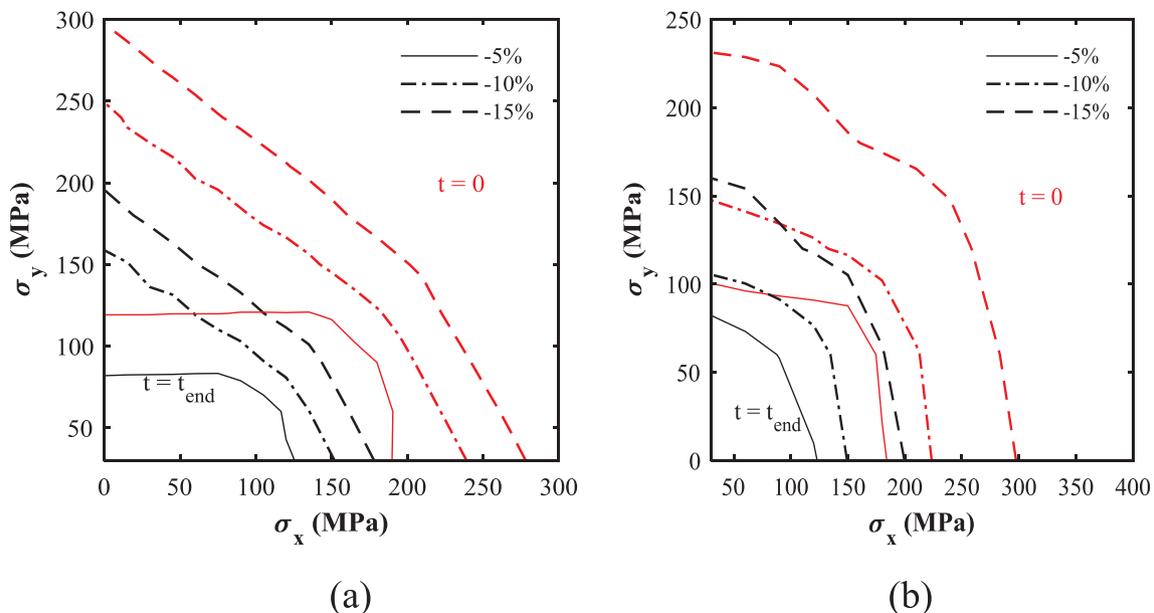
Fig. 8. The lines in the stiffness degradation contour map correspond to constant levels of stiffness loss before and after time-dependent deformation under biaxial loading of (a) $[0/90/\mp45]_s$ and (b) $[0/90]_s$ GFRP laminate.

under constant loading.

In Fig. 8(b), we have shown the stiffness degradation contour lines for the $[0/90]_s$ GFRP cross-ply, with the same ply properties as the $[0/90/\mp45]_s$ laminate. The contour lines correspond to 5%, 10% and 15% stiffness loss in either the axial, E_x^0, or transverse, E_y^0, modulus. Looking at the 5% stiffness loss line at time t = 0, we can see that the 5% stiffness degradation occurs at 175 MPa in the axial, and 100 MPa in the transverse direction. When viscoelastic deformation is taken into account (there is no viscoplasticity in the cross-ply because of the absence of shear stress), 5% stiffness degradation occurs at 125 MPa of axial load, and 75 MPa of transverse load. All the contour lines are slanted, due to the effect of transverse loading on crack multiplication. This can be explained by inspection of Fig. 6(b), where it can be seen that a transverse stress causes crack density in the 90° ply to increase, for a given axial load. In the case of the 0° ply, large transverse stresses cause an enhancement in crack density, leading to further stiffness degradation. As for the $[0/90/\mp45]_s$ laminate, the creep strains cause stiffness degradation contour lines to be shifted to much lower stresses; the shapes are also changed because of the creep strain deformation that occurs in the laminate.

4. Conclusions

A continuum damage mechanics-based SDM model was developed to incorporate the effects of viscoelastic-viscoplastic properties in GFRP laminates. Schapery's thermodynamics-based viscoelastic-viscoplastic constitutive model was implemented in the framework of the SDM model to investigate progressive damage by matrix micro-cracking in laminates. After initial validation with available experimental data, two GFRP laminates, namely $[0/90/\mp45]_s$ and $[0/90]_s$, were studied in this work. The damage behavior was predicted under an initial quasi-static step followed by viscoelastic-viscoplastic creep deformation under biaxial loading. The laminate was quasi-statically loaded up to the constant load level and then it was allowed to undergo creep at that constant load.

It was observed that the presence of a transverse load can increase the crack density compared to that under uniaxial loading. In the quasi-isotropic laminate, an increase of transverse load from 0 to 180 MPa with a constant longitudinal load of 210 MPa led to increase in crack density from 0.6 cr/mm to 1.5 cr/mm in the 45° ply. In the 90° ply, on the other hand, the crack density was barely affected when a transverse load is applied. For a $[0/90]_s$ cross-ply, a transverse load for a given axial load enhanced cracking in both plies.

The viscoelastic-viscoplastic deformation was found to reduce the micro-cracking initiation stress for both laminate stacking sequences. In the quasi-isotropic laminate, damage initiation was found at a uniaxial load of 140 MPa in longitudinal direction under quasi-static deformation. However, when viscoelastic-viscoplastic deformation was accounted for, the damage initiation in the laminate was at 80 MPa of longitudinal uniaxial load. In the case of the cross-ply, the crack initiation stress decreased from 150 MPa to 80 MPa when viscoelastic-viscoplastic deformation was taken into account. For both stacking sequences, an increase in transverse stress enhanced stiffness degradation.

To comprehensively quantify the damage under biaxial loading, stiffness degradation maps were developed under different combinations of axial and transverse loads. It was found that a given stiffness degradation occurs at lower axial loading levels when a transverse load is applied to the laminate. When the effect of creep was accounted for, the level of stiffness degradation for a given biaxial loading scenario was always more severe. Depending on the effect of transverse load on the evolution of damage in the different plies of the laminates, the slopes of the contour lines were different. Due to the extensive effects of viscoelastic-viscoplastic deformation in these composites, the contour lines describing the damage state after creep were shifted to lower loads, indicating more significant damage, and underwent changes in

their shape, due to the time-dependent evolution in creep strain.

Taken together, these results demonstrate the ability of the SDM model to predict time-dependent damage progression in viscoelastic-viscoplastic laminates under biaxial constant loading. Through its ability to accurately take into account biaxial loads, and to predict the time-dependent damage progression in individual plies, the model paves the way for the design of damage-tolerant composites structures which can withstand more demanding thermo-mechanical environments.

References

[1] Herakovich CT. Mechanics of fibrous composites; 1998.
[2] Orifici AC, Herszberg I, Thomson RS. Review of methodologies for composite material modelling incorporating failure. Compos Struct 2008;86(1–3):194–210.
[3] Gürdal Z, Haftka RT, Hajela P. Design and optimization of laminated composite materials. Wiley; 1999.
[4] Tuttle ME, Pasricha A, Emery AF. The nonlinear viscoelastic-viscoplastic behaviour of IM7/5260 composites subjected to cyclic loading. J Compos Mater 1995;29(15):2025–46.
[5] Ahci E, Talreja R. Characterization of viscoelasticity and damage in high temperature polymer matrix composites. Compos Sci Technol 2006;66(14):2506–19.
[6] Asadi A, Raghavan J. Influence of time-dependent damage on creep of multidirectional polymer composite laminates. Compos Part B Eng 2011;42(3):489–98.
[7] Nguyen TH, Gamby D. Effects of nonlinear viscoelastic behaviour and loading rate on transverse cracking in CFRP laminates. Compos Sci Technol 2007;67(3–4):438–52.
[8] Dillard DA, Morris DH, Brinson HF. Creep and creep rupture of laminated graphite/epoxy composites; 1980.
[9] Raghavan J, Meshii M. Time-dependent damage in carbon fibre-reinforced polymer composites. Compos Part A Appl Sci Manuf 1996;27:1223–7.
[10] Birur A, Gupta A, Raghavan J. Creep rupture of multidirectional polymer composite laminates—influence of time-dependent damage. J Eng Mater Technol 2006;128(4):611–7.
[11] Fitoussi J, Bocquet M, Meraghni F. Effect of the matrix behavior on the damage of ethylene-propylene glass fiber reinforced composite subjected to high strain rate tension. Compos Part B Eng 2013;45(1):1181–91.
[12] Talreja R, Singh CV. Damage and failure of composite materials. Cambridge University Press; 2012.
[13] Shen H, Yao W, Qi W, Zong J. Experimental investigation on damage evolution in cross-ply laminates subjected to quasi-static and fatigue loading. Compos Part B Eng 2017;120:10–26.
[14] Highsmith AL, Reifsnider KL. Stiffness-reduction mechanisms in composite laminates. Damage in composite materials: basic mechanisms, accumulation, tolerance, and characterization. ASTM International; 1982.
[15] Jagannathan N, Gururaja S, Manjunatha CM. Probabilistic strength based matrix crack evolution in multi-directional composite laminates. Compos Part B Eng 2016;87:263–73.
[16] Kashtalyan M, Soutis C. Modelling of stiffness degradation due to cracking in laminates subjected to multi-axial loading. Philos Trans R Soc A Math Phys Eng Sci 2016;374(2071):20160017.
[17] Hashin Z. Analysis of orthogonally cracked laminates under tension. J Appl Mech Trans ASME 1987;54(4):872–9.
[18] Sadeghi G, Hosseini-Toudeshky H, Mohammadi B. An investigation of matrix cracking damage evolution in composite laminates – development of an advanced numerical tool. Compos Struct 2014;108(1):937–50.
[19] Okabe T, Onodera S, Kumagai Y, Nagumo Y. Continuum damage mechanics modeling of composite laminates including transverse cracks. Int J Damage Mech 2017:1–19.
[20] Dvorak GJ, Laws N, Hejazi M. Analysis of progressive matrix cracking in composite laminates I. Thermoelastic properties of a ply with cracks. J Compos Mater 1985;19(3):216–34.
[21] Allen DH, Harris CE, Groves SE. A thermomechanical constitutive theory for elastic composites with distributed damage-I. Theoretical development. Int J Solids Struct 1987;23(9):1301–18.
[22] Williams KV, Vaziri R, Poursartip A. A physically based continuum damage mechanics model for thin laminated composite structures. Int J Solids Struct 2003;40(9):2267–300.
[23] Mandel U, Taubert R, Hinterhölzl R. Laminate damage model for composite structures. Compos Struct 2016;136:441–9.
[24] Salavatian M, Smith LV. An investigation of matrix damage in composite laminates using continuum damage mechanics. Compos Struct 2015;131:565–73.
[25] Läufer J, Becker V, Wagner W. Gradient enhancement of a transversely isotropic

continuum damage model. Compos Struct 2017;181:138–44.

[26] Singh CV, Talreja R. A synergistic damage mechanics approach for composite laminates with matrix cracks in multiple orientations. Mech Mater 2009;41(8):954–68.

[27] Montesano J, Singh CV. Predicting evolution of ply cracks in composite laminates subjected to biaxial loading. Compos Part B Eng 2015;75:264–73.

[28] Berton T, Montesano J, Singh CV. Development of a synergistic damage mechanics model to predict evolution of ply cracking and stiffness changes in multidirectional composite laminates under creep. Int J Damage Mech 2016;25(7):1060–78.

[29] Singh CV, Talreja R. A synergistic damage mechanics approach to mechanical response of composite laminates with ply cracks. J Compos Mater 2012;47:2475–501.

[30] Montesano J, Singh CV. A synergistic damage mechanics based multiscale model for composite laminates subjected to multiaxial strains. Mech Mater 2015;83:72–89.

[31] Ogi K, Takao Y. Evolution of transverse cracking in CF/Epoxy cross-ply laminates under creep loading. J Reinf Plast Compos 1999;18(13):1220–30.

[32] Ogi K, Smith PA. Modeling creep and recovery behavior of a quasi-isotropic laminate with transverse cracking. Adv Compos Mater 2002;11(1):81–93.

[33] Ogi K, Shiraishi T. Viscoelastic shear lag analysis of a cross-ply laminate with transverse cracking. The Japan society of mechanical engineers. 2001. p. 277–80.

[34] Asadi A. A model for time-independent and time-dependent damage evolution and their influence on creep of multidirectional polymer composite laminates; 2013.

[35] Varna J, Krasnikovs A, Kumar RS, Talreja R. A synergistic damage mechanics approach to viscoelastic response of cracked cross-ply laminates. Int J Damage Mech 2004;13(4):301–34.

[36] Giannadakis K, Varna J. Analysis of nonlinear shear stress–strain response of unidirectional GF/EP composite. Compos Part A Appl Sci Manuf 2014;62:67–76.

[37] Abu Al-Rub RK, Tehrani AH, Darabi MK. Application of a large deformation nonlinear-viscoelastic viscoplastic viscodamage constitutive model to polymers and their composites. Int J Damage Mech 2014;24(2):198–244.

[38] Montesano J, McCleave B, Singh CV. Prediction of ply crack evolution and stiffness degradation in multidirectional symmetric laminates under multiaxial stress states. Compos Part B Eng 2018;133:53–67.

[39] Sánchez-Heres LF, Ringsberg JW, Johnson E. Effects of matrix cracking on the estimation of operational limits of Frp laminates. In: 15th European conference on composite materials; 2012. pp. 1–8.

[40] Asadi A, Raghavan J. Model for prediction of simultaneous time-dependent damage evolution in multiple plies of multidirectional polymer composite laminates and its influence on creep. Compos Part B Eng 2015;79:359–73.

[41] Shokrieh MM, Omidi MJ. Tension behavior of unidirectional glass/epoxy composites under different strain rates. Compos Struct 2009;88(4):595–601.

[42] Schapery RA. On the characterization of nonlinear viscoelastic materials. Polym Eng Sci 1969;9(4):295–310.

[43] Megnis M, Varna J. Micromechanics based modeling of nonlinear viscoplastic response of unidirectional composite. Compos Sci Technol 2003;63(1):19–31.

[44] Rubenis O, Sparniņš E, Andersons J, Joffe R. The effect of crack spacing distribution on stiffness reduction of cross-ply laminates. Appl Compos Mater 2007;14(1):59–66.